Biological ferrous sulfate oxidation by *A. ferrooxidans* immobilized on chitosan beads

A. Giaveno [a,*], L. Lavalle [a], E. Guibal [b], E. Donati [c]

[a] *Facultad de Ingeniería, Universidad Nacional del Comahue, Buenos Aires 1400, (8300) Neuquén, Argentina*
[b] *École des Mines d'Alès, Laboratorie Génie de l'Environnement Industriel, Alès cedex, France*
[c] *CINDEFI (CONICET-UNLP), Facultad de Ciencias Exactas, 47 y 115 (1900) La Plata, Argentina*

Abstract

The immobilization of *Acidithiobacillus ferrooxidans* cells on chitosan and cross-linked chitosan beads and the biooxidation of ferrous iron to ferric iron in a packed-bed bioreactor were studied. The biofilm formation was carried out by using a glass column reactor loaded with chitosan or cross-linked chitosan beads and 9 K medium previously inoculated with *A. ferrooxidans* cells. The immobilization cycles on the carrier matrix with the bioreactor operating in batch mode were compared. Then, the reactor was operated using a continuous flow of 9 K medium at different dilution rates. The results indicate that the packed-bed reactor allowed increasing the flow rate of medium approximately two fold (chitosan) and eight fold (chitosan cross-linked) without cells washout, compared to a free cell suspension reactor used as control, and to reach ferric iron productivities as high as 1100 and 1500 mg l^{-1} h^{-1} respectively.

Scanning electron microscopy micrographs of the beads, infrared spectroscopy and the X-ray diffraction patterns of precipitates on the chitosan beads were also investigated.

Keywords: *Acidithiobacillus ferrooxidans*; Iron oxidation; Packed-bed bioreactor; Chitosan carrier

1. Introduction

Acidithiobacillus ferrooxidans is an acidophilic bacterium capable of oxidizing different inorganic compounds, the most common of which is ferrous sulfate. *A. ferrooxidans* is one of the dominant microorganisms not only in the bioleaching of minerals but also in the pretreatment (biooxidation) of refractory gold. Both processes imply the oxidation of sulfide by ferric iron; the resultant ferrous iron is re-oxidized to the ferric state by the bacteria. The bioproduction of ferric iron has been also employed to desulfurize gases containing hydrogen sulfide or sulfur dioxide, in the desulfurization of coal and even in the treatment of acid mine drainages (Rohwerder et al., 2003; Rawlings et al., 2003; Watling, 2006; Akcil et al., 2007).

In all those cases, large volumes of ferric iron solutions should be generated. The use of free cells has a limited potential because biomass has low physical strength and low density causing serious problems to be separated from the solution. Cell immobilization provides several advantages in protecting the cells from hostile environments and maintaining higher cellular metabolic activities and increasing the value of dilution rate where the washout takes place.

The natural tendency of *A. ferrooxidans* to grow on surfaces not only on inert support but also on minerals makes it an adequate microorganism for cell immobilization and useful to increase iron(III) productivity (Karamanev and Nikolov, 1988; Ramírez et al., 1997; Harneit et al., 2006). Several supports have been employed, including the use of glass beads, activated carbon particles, sand, polystyrene, polyurethane, poly (vinyl alcohol), calcium alginate, ion-exchange resin, nickel alloy fibre, PVC and diatomaceous earth (Grishin and Tuovinen, 1988; Armentia and Webb, 1992; Porro et al., 1993; Wakao

* Corresponding author. Tel.: +54 299 4490300 456; fax: +54 299 4490300 286.
E-mail address: agiaveno@uncoma.edu.ar (A. Giaveno).

et al., 1994; Mazuelos et al., 1999; Gomez et al., 2000; Curutchet et al., 2001; Mesa et al., 2002, 2004; Long et al., 2003, 2004a,b; Park et al., 2005; Giro et al., 2006; Yujian et al., 2006; Mousavi et al., 2007; Yujian et al., 2007). In many of those cases, *A. ferrooxidans* cells immobilized could grow at higher dilution rates reaching high iron(III) productivity. Additionally, cells were retained in the support matrix leaving the ferric iron solution almost cell free.

Some materials of biological origin exhibit very high sorption capacities. Chitosan has proved to be very efficient for the recovery of several toxic and strategic metals (Guibal, 2004), or dyes (Guibal et al., 2005). Chitosan results from the alkaline deacetylation of chitin, one of the most abundant polysaccharides in Nature after cellulose. It is commercially produced from shrimp and crab shells. In most cases (partial deacetylation) the biopolymer can be considered as a heteropolymer constituted of acetylglucosamine and glucosamine units. The biopolymer is characterized by its high percentage of nitrogen, present under the form of amine groups that are responsible for the binding of metal cations through chelation mechanisms. Glutaraldehyde has been frequently used to cross-link chitosan and to stabilize it in acidic solutions. The reaction occurs through a Schiff's base reaction between aldehyde groups of the cross-linker and some amine groups of chitosan. The chemical modification of the biopolymer may be used to increase the sorption efficiency but also to improve sorption selectivity and to decrease the sensitivity to environmental parameters (Guibal, 2004). Chitosan has been employed as support for cell immobilization during the last decade (Tartakovsky et al., 1998; Freeman et al., 1999; Ravi Kumar, 2000; Öztop et al., 2002; Peniche et al., 2003; Freeman and Dror, 2004; Selezneva et al., 2006; Wang and Chao, 2006; Vignoli et al., 2006).

In the present study the immobilization of *A. ferrooxidans* cells on chitosan and cross-linked chitosan beads and the biooxidation of ferrous iron to ferric iron in a packed-bed bioreactor were studied.

2. Materials and methods

2.1. Microorganism and cultivation

A strain of *A. ferrooxidans* from Santa Rosa de Arequipa (DSM11477) was used throughout these experiments. The microorganism was grown and maintained on 9 K medium at initial pH 1.80 (Jensen and Webb, 1995).

2.2. Chitosan and cross-linked chitosan materials

Chitosan was supplied by France Chitine (France) as flaked material. The biopolymer was characterized by a degree of acetylation of 13% and a molecular weight of 125,000 g mol^{-1}. Gel beads were prepared using a two-step procedure consisting in: (a) chitosan dissolving in acetic acid solution (2.5% w/w of chitosan in acetic acid solution respecting the equimolarity between amine groups and acetic acid), followed by (b) the distribution of the viscous solution through a thin nozzle (0.8 μm, internal diameter) into a neutralizing alkaline bath (1 M NaOH solution). The alkaline solution contributed both to neutralizing the acidity of chitosan solution and to gelling the beads. A spherical shape was assumed for each particle, and the arithmetic mean of the diameters of each bead was used for the surface area and volume of the carrier calculations. The diameter of the beads was measured close to 1.8 mm (±0.2 mm). Water content was close to 96%.

Being chitosan soluble in most mineral and organic acids, with the exception of sulfuric acid, it must be cross-linked when the biopolymer is used in inappropriate acidic solutions. Several processes have been discussed in the literature; the glutaraldehyde cross-linking seems to be the most resistant to acidic environments. The reaction proceeds through a Schiff's base reaction between amine groups of chitosan and aldehyde functions of the cross-linking agent, contributing to the formation of imine linkages between polymer chains. The supplementary linkages cause polymer stabilization in acidic media. Chitosan cross-linking with glutaraldehyde was performed by mixing for 16 h a known amount of chitosan with an equimolar quantity of glutaraldehyde (50% v/v) in a large volume of demineralized water to obtain fluid slurry. The equimolar quantity of glutaraldehyde was calculated taking into account the deacetylation of chitosan: the equimolarity is based on the number of free amine groups of the biopolymer. After cross-linking treatment the solid was separated and washed several times with water to remove the unreacted glutaraldehyde. The size of the beads was not significantly changed by the cross-linking treatment. Gel beads were then dried at 50 °C for 16 h.

2.3. Bacterial growth in the presence of chitosan

200 chitosan or cross-linked chitosan beads (1.0 g of dried carrier) were added to 250 ml Erlenmeyer flasks containing 100 ml of 9 K medium (pH 1.80) inoculated with *A. ferrooxidans* cells. Initial bacterial population was 1.2×10^7 cells ml^{-1}. The flasks were incubated at 30 °C and 180 rpm. Inoculated controls without chitosan were also carried out.

2.4. Process of biofilm formation

The biofilm formation was carried out in a packed-bed reactor. The device was based on a glass column with an inner diameter of 2.5 cm and a high of 25.0 cm with inlets for fresh medium and air at the bottom. The outlet for effluent and exhaust air was at the top of the column. The reactor was loaded with 2500 chitosan or cross-linked chitosan beads (12.5 g of dried carrier with an estimated volume and surface area close to 10.5 cm^3 and 314.0 cm^2 respectively). Additionally, the reactor was filled with 100 ml of the 9 K medium (pH 1.80) previously inoculated with *A. ferrooxidans* cells. An air flow of 72.0 l h^{-1} was supplied to add the gaseous nutrients. The reactor working volume (V_t) considered for further calculations was 100 ml although the total volume occupied in the reactor consisted in the sum of several volumes (the 9 K fresh medium volume, the total carriers volume, the total fixed film volume and the total volume of air bubbles within the reactor).

In order to allow a fixed biofilm formed on the carrier matrix the reactor was operated in batch mode. When ferrous iron was completely oxidized, medium was replaced by fresh medium without any additional inoculation. After several of these consecutive batch cycles it was considered that the biofilm behavior was properly in place to switch the reactor to a continuous flow. In this mode of operation the flow rates for fresh media (F) were regulated with peristaltic pumps from 4 to 80 ml h^{-1} in order to obtain different dilution rates (D) ranged between values of 0.01 and 0.8 h^{-1}. Steady state conditions were used at each flow rate for estimating the kinetics of ferrous sulfate oxidation. After modifying the flow rate, we assumed that no further change in the iron oxidation rate for three residence times ($\tau = D^{-1}$) indicated that steady state had been reached. All these experiments were conducted in duplicate.

2.5. Analytical procedures

Ferrous iron concentration was measured by titration with potassium permanganate. Total soluble iron was determined by atomic absorption spectrophotometry. The bacterial populations (free in solution) were quantified using a Petroff Hausser counting chamber in a phase-contrast microscope. Both kinds of chitosan beads were analyzed by means of scanning electron microscopy (SEM) before and after cell immobilization in order to compare these materials, to detect the changes in their surfaces and study the morphological aspect of the precipitates at the end of the tests. The beads were removed from the columns; they were dried at 50 °C for 2 h and then they were glued onto a brass mount. The specimens were gold coated before SEM examination. Scanning electron micrographs of the beads were taken in a Philips 515 equipment.

Biofilm was studied by infrared spectroscopy in a Buck 500 spectrophotometer using KI pellet technique with 3 mg of the sample suspended in a transparent disc of 300 mg of KI. The pellet was formed in a dye under high pressure. Additionally, the biofilms were examined by X-ray diffraction in order to identify the precipitates formed on the bead surfaces. For XRD analysis the chitosan beads were withdrawn from the reactor at the end of the test and then the samples were air-dried, ground, and analyzed using a Rigaku DII-Max automated diffractometer between 5–70° 2 θ with Cu–Kα radiation at 2°/min rate.

3. Results and discussion

3.1. Evaluation of chitosan beads as carrier for A. ferrooxidans inmobilization

Fig. 1 shows the results obtained during *A. ferrooxidans* growth in the presence of chitosan and cross-linked chitosan beads. It can be seen that ferrous iron oxidation (Fig. 1A) was not affected by the presence of chitosan beads and was slightly slower in the presence of cross-linked chitosan. On the other hand Fig. 1B shows that the highest productivity of ferric iron was observed in the culture with chitosan (200 mg l^{-1} h^{-1}) while the culture with cross-linked chitosan reached the lowest value (170 mg l^{-1} h^{-1}). The possible bacterial inhibition shown in the last culture could be explained by the presence of little amounts of glutaraldehyde that causes the attachment cell to cell. This is in agreement with large chains of cells observed in the culture with cross-linked chitosan and not in the others. As it can be expected, cell populations in suspension were lower in the presence of chitosan or cross-linked chitosan due to the bacterial attachment to the solids. The high biooxidation rate of

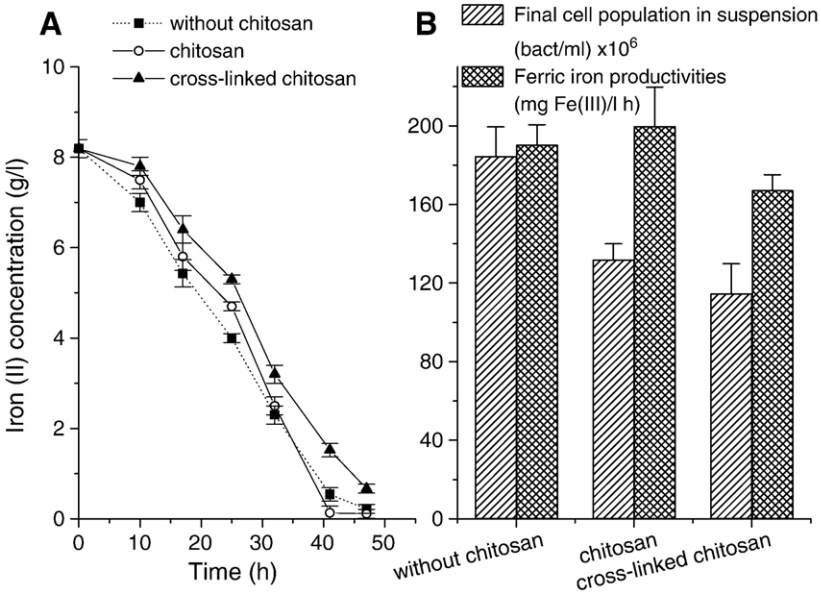


Fig. 1. *A. ferrooxidans* growth in the presence of chitosan and cross-linked chitosan beads. (A) Ferrous iron concentration versus time. (B) Final cell population in suspension and ferric iron productivities.

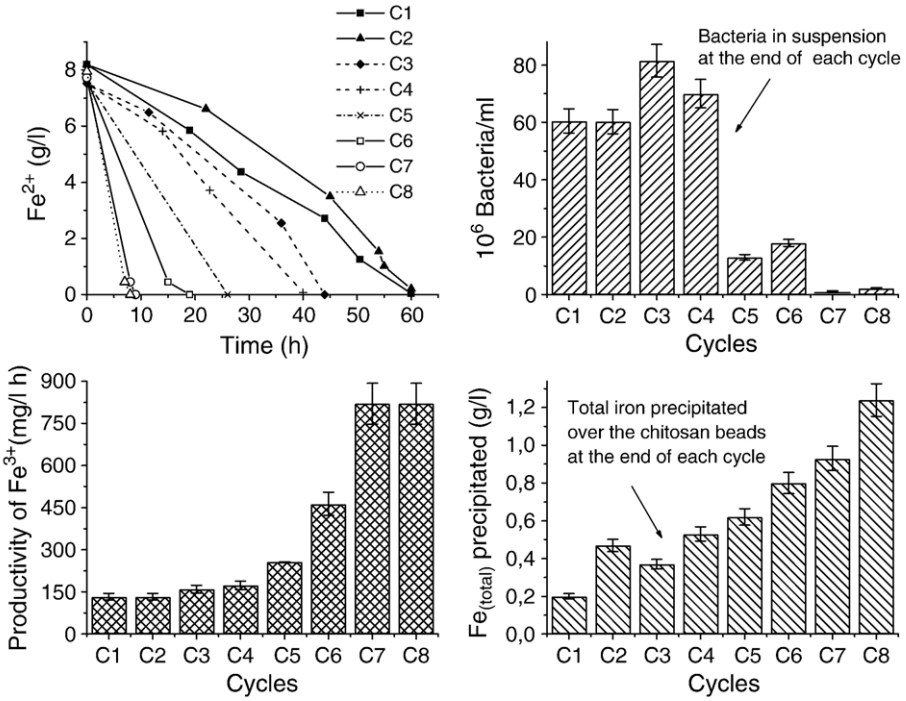


Fig. 2. Ferrous iron evolution along each isothermal colonization cycle and final values of free cell population, ferric iron productivity and total iron precipitated over the cross-linked chitosan beads.

ferrous iron in the presence of the biopolymer at level comparable to the control justify using gel beads as a possible support.

3.2. Ferrous iron oxidation in repeated batch culture of chitosan beads

In order to obtain a biofilm in the bioreactors containing chitosan and cross-linked chitosan, several isothermal colonization cycles were carried out using 9 K medium at pH 1.80. Fig. 2 shows the performance of the bioreactor loaded with cross-linked chitosan beads which was similar to that observed for untreated chitosan beads.

Along the different steps, both the rate of ferrous iron oxidation and the ferric iron productivity were increasing while the free cell concentration was decreasing until reaching a constant value. The time needed to oxidize all the substrate in the last batch cycle was nearly ten fold lower than in the first one. The maximum iron(II) biooxidation rate of 820 mg l^{-1} h^{-1} is comparable with most values reported in literature and even higher than many of them (Nikolov et al., 2002; Long et al., 2004a). The cell retention after 6 cycles was almost complete while iron precipitation increased continuously during the process of biofilm formation. These facts could suggest that iron precipitation contributes to cell immobilization, which is in agreement to the data reported by Pogliani and Donati (2000).

3.3. Continuous oxidation of ferrous iron in packed-bed bioreactor

At this moment, it was possible to operate the reactor using a continuous flow of 9 K medium at different dilution rates. Fig. 3 shows the iron (III) productivity as a function of the dilution rate (D) for both carriers. The packed-bed reactor allowed increasing the flow rate of medium approximately two fold (untreated chitosan) and eight fold (cross-linked chitosan) without cells washout, compared to a free cell suspension reactor used as control. The advantage of continuous operation systems is reaching higher productivity values than those obtained in the batch mode. The highest ferrous iron oxidation rates were 1100 and 1500 mg l^{-1} h^{-1} for untreated chitosan and cross-linked chitosan, respectively. These maximum rates achieved using 12.5 g of support are comparable with most values reported in the literature and higher than many of them. It is possible to compare the performance of chitosan beads as carrier which was achieved in this study with regard to different packed and

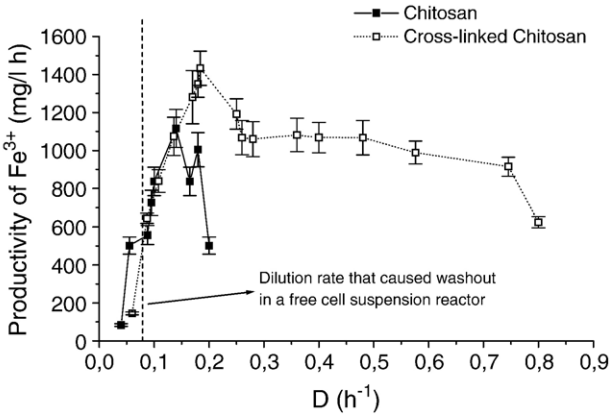


Fig. 3. Productivity of iron (III) in continuous packed-bed reactor using chitosan and cross-linked chitosan beads.

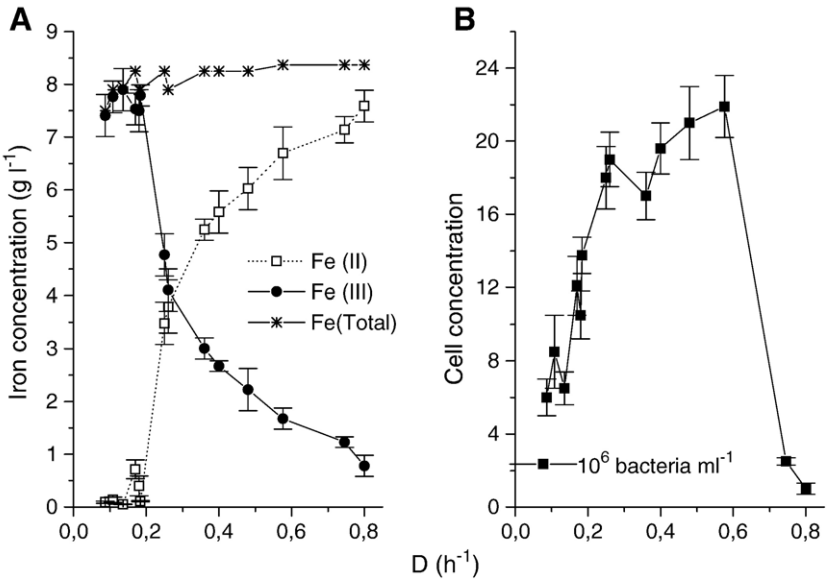


Fig. 4. The iron and cell concentrations in the outlet flow reactor loaded with cross-linked chitosan beads.

fluidized bed reactors with glass and resin beads and activated carbon tested by Grishin and Tuovinen (1988). Taking into account the total matrix surface in each reactor the specific productivity of ferrous iron oxidation reached in this study by chitosan beads was higher than the glass beads in a packed-bed reactor flow and activated carbon in a fluidized bed reactor. Only activated carbon in a packed-bed reactor showed to be more efficient than both kinds of chitosan beads. It was also observed that the higher the dilution rate, the lower the iron(III) precipitation. This fact is coincident with the behavior of both iron(II) and iron(III) concentrations in the outlet flow reactor (Fig. 4A). The total iron concentration slightly increases with the dilution rate. Additionally, in Fig. 4B it is possible to see the evolution of the cell concentration in the outlet flow reactor and to estimate the dilution rate that caused the reactor washout.

3.4. Chitosan beads and biofilm characterization

Fig. 5 shows the scanning electron micrographs of the surfaces of chitosan (A) and cross-linked chitosan beads (B). It can be seen that the surface of treated beads is more wrinkled than that of untreated beads. Probably this characteristic allowed operating the bioreactor at higher dilution rates.

Fig. 6 shows the infrared spectra of the beads before and after bacterial colonization indicating significant changes. From the chitosan spectrum before bacterial colonization, it can be found that peaks 1 to 3 are the distinctive absorption bands at 1662 cm^{-1} (Amide I), 1598 cm^{-1} ($-NH_2$ bending) and 1380 cm^{-1} (Amide III). While peaks 4–6 represent the absorption bands at 1156 cm^{-1} (anti-symmetric stretching of the C–O–C bridge), the peaks at 1075 and 1033 cm^{-1} (skeletal vibration involving the C–O stretching) are characteristics of the saccharidic (h) structure. Additionally, it is expected to find a broader band near 3300 to 3600 cm^{-1} (peak 7) that corresponds to H_2O vibrations (Peniche et al., 1999; Brugnerotto et al., 2001; Zhang et al., 2003).

After colonization, it was possible to identify the most distinctive IR absorbance frequencies of jarosite (ferric iron sulfate) which are also shown in Fig. 6. From the transmittance spectra of jarosite, the band 8 is primarily due to the structural

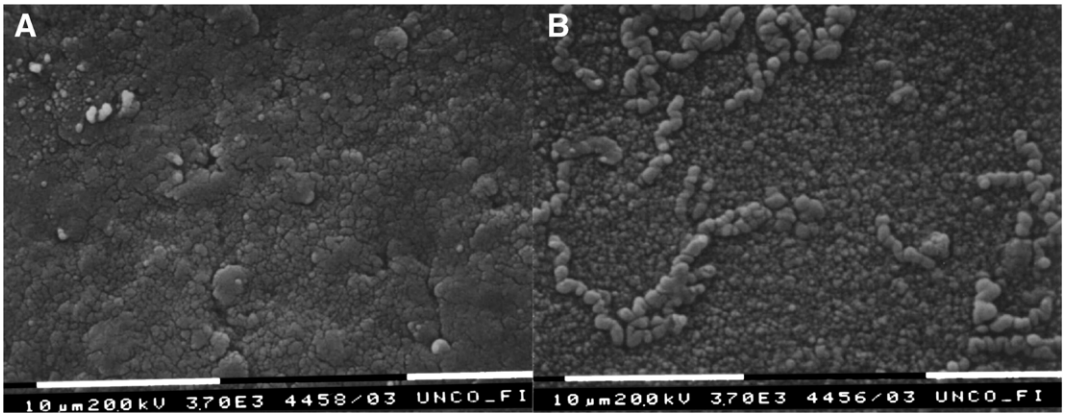


Fig. 5. Scanning electron micrograph for chitosan (A) and cross-linked chitosan beads (B). Note: Bar size = 10 µm.

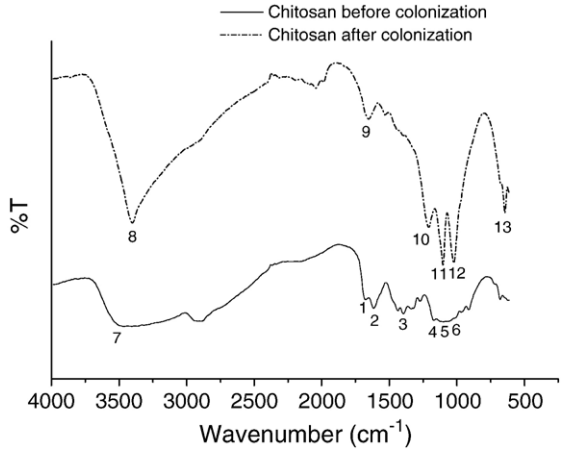


Fig. 6. IR spectra for chitosan beads before and after colonization. The peaks 1–7 are the distinctive absorption bands used to characterize this saccharide structure. The peaks 8–13 show the absorption bands detected after colonization most of them belong to the jarosite spectrum.

OH stretching mode and includes water modes as well, specially for synthetic samples. The peak 9, at 1648 cm^{-1}, is in agreement with the band recorded in jarosite spectrum in the range between 1630 and 1650 cm^{-1}, which was assigned to water deformation. This band was even observed after prolonged drying acetone-washed samples under vacuum at 80–100 °C. The strongest bands (peaks 10 and 11) are due to the $\vee 3$ (SO_4^{2-}) stretching vibration and are observed as a doublet near 1100 and 1200 cm^{-1}. Other peaks were identified in this IR spectrum; one of them (12) is a band due to $\vee_1$ (SO_4^{2-}) vibrations. The other peak (13) is observed near 1000 cm^{-1} for jarosite and it is corresponding to $\vee_1$ (SO_4^{2-}) while that another strong doublet is observed near 625 and 660 due to $\vee_4$ (SO_4^{2-}) bending vibration (Lazaroff et al., 1982; Sasaki and Konno, 2000; Bishop and Murad, 2005).

In bioreactors to produce ferric iron, jarosite precipitation is an unwanted phenomenon due to the diminishment of the diffusion of reactants and products through the layer of deposits and the blockage of pumps and valves. However, jarosite deposits participate in the process of biofilm formation (Pogliani and Donati, 2000; Daoud and Karamanev, 2006). After the first and reversible phase of cell adhesion, jarosite precipitation builds the biofilm matrix. These deposits on the surface would allow the later adsorption of cells on the pores and the formation of the biofilm. That is why the best performance for this kind of bioreactors is shown by support matrices with high initial cell adherence and/or high porosity. These supports can allow fast oxidation of ferrous iron very close to the surface increasing pH and ferric iron concentration and the subsequent jarosite precipitation. As the formation of

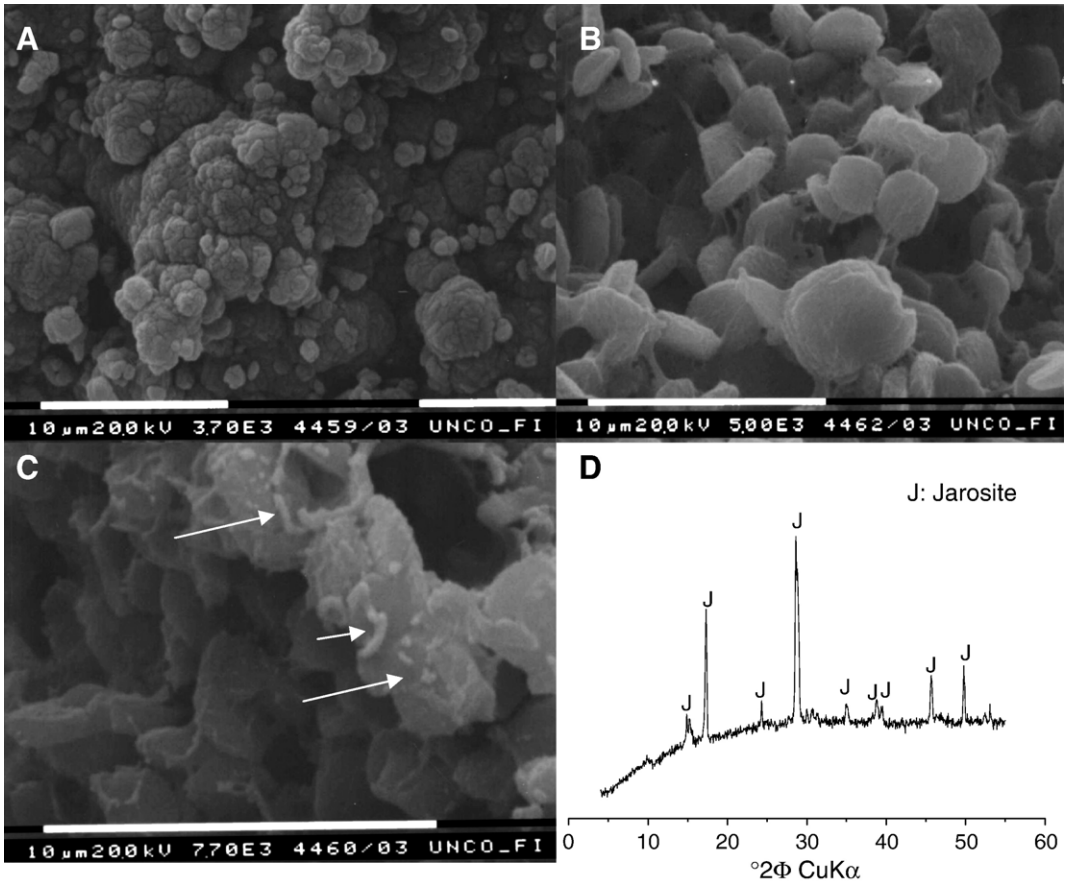


Fig. 7. A) Scanning electron micrograph of jarosite precipitation on cross-linked chitosan beads collected from the reactor after the test. Images B) and C) show the SEM micrographs taken from the inside of the same chitosan beads. Some characteristic jarosite crystals can be distinguished and the arrows could indicate some bacteria trapped into the biofilm. Note: Bar size = 10 µm D) X-ray diffraction pattern which allow identifying the jarosite precipitates.

jarosite is mainly dependent on pH, it has been reported that pH values between 1.6 and 1.8 are adequate not only to maintain high ferrous iron oxidation rates but also enough amounts of ferric precipitates for a good biofilm (Pogliani and Donati, 2000).

The three SEM micrographs in Fig. 7 show the outside (A) and the inside (B and D) of the cross-linked chitosan beads collected from the reactor after the precipitation of the ferric hydroxysulfates. The shape of the precipitates shown in Fig. 7A and the occurrence of the characteristic crystals that can be distinguished in Fig. 7B and C are consistent with the data reported by several authors from jarosite precipitation carried out in acidic conditions (Lazaroff et al., 1982; Grishin and Touvinen, 1988; Sasaki and Konno, 2000; Cadena et al., 2006). On the other hand, the arrows drawn in Fig. 7C indicates the presence of some bacteria trapped into the biofilm.

The XRD patterns shown in Fig. 7D indicate that jarosite is the main product precipitated on the chitosan beads and there is not evidence of other crystalline by-products co-precipitated. Moreover, from the XRD spectrum obtained it is possible to identify the most representative diffraction bands belonging to jarosite mineral (Grishin and Touvinen, 1988; Stahl et al., 1993; Sasaki and Konno, 2000; Kawano and Tomita, 2001; Paktunc and Dutrizac, 2003).

4. Conclusions

A. ferrooxidans cells were immobilized successfully in chitosan and cross-linked chitosan beads. The packed-bed reactor allowed increasing the flow rate of medium approximately two fold (chitosan untreated) and eight fold (chitosan cross-linked) without cells washout, compared to a free cell suspension reactor used as control, and to reach ferric iron productivities as high as 1100 and 1500 mg l^{-1} h^{-1} respectively. Differences found in the performance of continuous bioreactor using untreated chitosan and cross-linked chitosan could be attributed to a more wrinkled bead surface in the last case. It was possible to identify the most distinctive peaks of jarosite in the infrared spectra and in the XRD patterns from the precipitates produced after colonization which could play an important role during biofilm formation.

Acknowledgement

This work has been supported by Facultad de Ingeniería, Universidad Nacional del Comahue, partially by ANPCyT (PICT 25300) and CONICET (PIP 5147) from Argentina. Alfa Programme (Contract number AML/190901/06/18414/II-0548-FC-FA) is also gratefully acknowledged.

References

Akcil, A., Ciftci, H., Deveci, H., 2007. Role and contribution of pure and mixed cultures of mesophiles in bioleaching of a pyritic chalcopyrite concentrate. Miner. Eng. 20, 310–318.

Armentia, H., Webb, C., 1992. Ferrous sulphate oxidation using *Thiobacillus ferrooxidans* cells immobilised in polyurethane foam support particles. Appl. Microbiol. Biotechnol. 36, 697–700.

Bishop, J., Murad, E., 2005. The visible and infrared spectral properties of jarosite and alunite. Am. Mineral. 90, 1100–1107.

Brugnerotto, J., Lizardi, J., Goycoolea, F., Argüelles-Monal, J., Desbrières, W., Rinaudo, M., 2001. An infrared investigation in relation with chitin and chitosan characterization. Polymer 42, 3569–3580.

Cadena, J., Chimenos, J., Queralt, I., Viladevall, M., Flores, K., Pérez, F., 2006. Efecto del mineral de ganga en la síntesis de jarosita de potasio y su distribución de tamaños de partícula. Boletín de Mineralogía 17, 21–28.

Curutchet, G., Donati, E., Oliver, C., Pogliani, C., Viera, M., 2001. Development of *Thiobacillus* biofilm for metal recovery. In: Doyle, R.J. (Ed.), Microbial Growth in Biofilms, Part B: Special Environments and physicochemical aspects. Methods in Enzymology, vol. 337. Academic Press, San Diego, pp. 171–186.

Daoud, J., Karamanev, D., 2006. Formation of jarosite during Fe^{2+} oxidation by *Acidithiobacillus ferrooxidans*. Miner. Eng. 19, 960–967.

Freeman, A., Dror, Y., 2004. Immobilization of disguised yeast in chemically crosslinked chitosan beads. Biotechnol. Bioeng. 44 (9), 1083–1088.

Freeman, A., Abramov, S., Georgiou, G., 1999. Site-protected fixation and immobilization of Escherichia coli displaying surface-anchored beta-lactamase. Biotechnol. Bioeng. 62 (2), 155–159 20.

Giro, M.E.A., García Jr., O., Zaiat, M., 2006. Immobilized cells of *Acidithiobacillus ferrooxidans* in PVC strands and sulfite removal in a pilot-scale bioreactor. Biochem. Eng. J. 28, 201–207.

Gomez, J.M., Cantero, D., Webb, C., 2000. Immobilization of *Thiobacillus ferrooxidans* cells on nickel alloy fibre for ferrous sulphate oxidation. Appl. Microbiol. Biotechnol. 54, 335–340.

Grishin, S.I., Tuovinen, O.H., 1988. Fast kinetics of Fe^{2+} oxidation in packed-bed reactors. Appl. Environ. Microbiol. 54, 3092–3100.

Guibal, E., 2004. Metal ion interactions with chitosan — a review. Separ. Purif. Technol. 38 (1), 43–74.

Guibal, E., Touraud, E., Roussy, J., 2005. Chitosan interactions with metal ions and dyes: dissolved-state versus solid-state application. World J. Microbiol. Biotechnol. 21 (6–7), 913–920.

Harneit, K., Göksel, A., Kock, D., Klock, J.H., Gehrke, T., Sand, W., 2006. Adhesion to metal sulphide surfaces by cells of *Acidithiobacillus ferrooxidans, Acidithiobacillus thiooxidans* and *Leptospirillum ferrooxidans*. Hydrometallurgy 83, 245–254.

Jensen, A.B., Webb, C., 1995. Ferrous sulfate oxidation using *Thiobacillus ferrooxidans:* a review. Process Biochem. 30, 225–236.

Karamanev, D.G., Nikolov, L.N., 1988. Influence of some physicochemical parameters on bacterial activity of biofilm: ferrous iron oxidation by *Thiobacillus ferrooxidans*. Biotechnol. Bioeng. 31, 295–299.

Kawano, M., Tomita, K., 2001. Geochemical modelling of bacterially induced mineralization of schwertmannite and jarosite in sulfuric acid spring water. Am. Mineral. 86, 1156–1165.

Lazaroff, N., Sigal, W., Wasserman, A., 1982. Iron oxidation and precipitation of ferric hydroxysulfates by resting *Thiobacillus ferrooxidans* cells. Appl. Environ. Microbiol. 43 (4), 924–938.

Long, Z., Huang, Y., Cai, Z., Cong, W., Ouyang, F., 2003. Biooxidation of ferrous iron by immobilized *Acidithiobacillus ferrooxidans* in poly(vinyl alcohol) cryogel carriers. Biotechnol. Lett. 25, 245–249.

Long, Z., Huang, Y., Cai, Z., Cong, W., Ouyang, F., 2004a. Immobilization of *Acidithiobacillus ferrooxidans* by a PVA–boric acid method for ferrous sulphate oxidation. Process Biochem. 39, 2129–2933.

Long, Z., Huang, Y., Cai, Z., Cong, W., Ouyang, F., 2004b. Kinetics of continuous ferrous iron oxidation by *Acidithiobacillus ferrooxidans* immobilized in poly (vinyl alcohol) cryogel carriers. Hydrometallurgy 74, 181–187.

Mazuelos, A., Palencia, I., Romero, R., Rodriguez, G., Carranza, F., 1999. Design variables in high efficiency reactors for the biooxidation of ferrous iron in solution. In: Amils, R., Ballester, A. (Eds.), Biohydrometallurgy and the environment toward the mining of the 21st century. Elsevier, Amsterdam, pp. 501–510.

Mesa, M., Macías, M., Cantero, D., 2002. Mathematical model of the oxidation of ferrous iron by a biofilm of *Thiobacillus ferrooxidans*. Biotechnol. Prog. 18, 679–685.

Mesa, M., Andrades, J., Macías, M., Cantero, D., 2004. Biological oxidation of ferrous iron: study of bioreactor efficiency. J. Chem. Technol. Biotechnol. 79, 163–170.

Mousavi, S., Yaghmaei, S., Jafari, A., 2007. Influence of process variables on biooxidation of ferrous sulphate by an indigenous *Acidithiobacillus ferrooxidans*. Part II: Bioreactor experiments. Fuel 86, 993–999.

Nikolov, L., Karamanev, D., Mamatarkova, V., Mehochev, D., Dimirov, D., 2002. Properties of *Thiobacillus ferrooxidans* formed in rotating biological contactor. Bioch. Eng. J. 12, 43–48.

Öztop, H.N., Saraydin, D.Ç., Etinus, S., 2002. pH-sensitive chitosan films for baker's yeast immobilization. Appl. Biochem. Biotechnol. 101 (3), 239–250.

Paktunc, D., Dutrizac, J., 2003. Characterization of arsenate for sulfate substitution in synthetic jarosite using X-ray diffraction and X-ray absorption spectroscopy. The Can. Mineral. 41, 905–919.

Park, D., Lee, D., Joung, J., Park, J., 2005. Comparison of different bioreactor systems for indirect H_2S removal using iron-oxidizing bacteria. Process Biochem. 40, 1461–1467.

Peniche, C., Arguelles-Monal, W., Davidenko, N., Sastre, R., Gallardo, A., San Roman, J., 1999. Self-curing membranes of chitosan/PAA IPNs obtained by radical polymerization: preparation, characterization and interpolymer complexation. Biomaterials 20, 1869–1878.

Peniche, C., Argüelles-Monal, W., Peniche, H., Acosta, N., 2003. Chitosan: an attractive biocompatible polymer for microencapsulation. Macromol. Biosci. 3 (10), 511–520.

Pogliani, C., Donati, E., 2000. Immobilization of *Thiobacillus ferrooxidans:* importance of jarosite precipitation. Process Biochem. 35, 997–1004.

Porro, S., Pogliani, C., Donati, E., Tedesco, P.H., 1993. Use of packed bed bioreactors. Application to ores bioleaching. Biotechnol. Lett. 15, 207–212.

Ramírez, S., Reche, C., Curutchet, G., Alonso, S., Donati, E., 1997. Bacterial attachment: its role in bioleaching processes. Process Biochem. 32, 573–578.

Ravi Kumar, M.N.V., 2000. A review of chitin and chitosan applications. React. Funct. Polym. 46, 1–27.

Rawlings, D., Dew, D., du Plessis, C., 2003. Biomineralization of metal-containing ores and concentrates. Trends Biotechnol. 21, 38–44.

Rohwerder, T., Gehrke, T., Kinsler, K., Sand, W., 2003. Bioleaching review. Part A: Progress in bioleaching: fundamentals and mechanisms of bacterial metal sulfide oxidation. Appl. Microbiol. Biotechnol. 63, 239–248.

Sasaki, K., Konno, H., 2000. Morphology of jarosite-group compounds precipitated from biologically and chemically oxidized Fe ions. The Can. Mineral. 38, 45–56.

Selezneva, I., Savintseva, I., Vikhlyantseva, E., Davydova, G., Gavrilyuk, B., 2006. Immobilization and long-term culturing of mouse embryonic stem cells in collagen–chitosan gel matrix. Bull. Exp. Biol. Med. 142 (1), 119–122.

Stahl, R., Fanning, D., James, B., 1993. Goethite and jarosite precipitation from ferrous sulphate solutions. Soil Sci. Soc. Am. J. 57, 280–282.

Tartakovsky, B., Petti, L., Hawari, J., Guiot, S., 1998. Immobilization of anaerobic sludge using chitosan crosslinked with lignosulfonate. Ind. Microbiol. Biotechnol. 20 (1), 45–47.

Vignoli, J., Colabone Celligoi, M., Ferreira da Silva, R., de Barros, M., 2006. The production of sorbitol by permeabilized and immobilized cells of *Z. mobilis* in sucrose. Braz. Arch. Biol. Technol. 49, 683–687.

Wakao, N., Endo, K., Mino, K., Sakural, Y., Shiota, H., 1994. Immobilization of *Thiobacillus ferrooxidans* using various polymers as matrix. J. Gen. Appl. Microbiol. 40, 249–358.

Wang, J.Y., Chao, J.Y., 2006. Immobilization of cells with surface-displayed chitin-binding domain. Appl. Environ. Microbiol. 72 (1), 927–931.

Watling, H.R., 2006. The bioleaching of sulphide minerals with emphasis on copper sulphides — a review. Hydrometallurgy 84, 81–108.

Yujian, W., Xiaojuan, Y., Hongyu, L., Wei, T., 2006. Immobilization of *Acidithiobacillus ferrooxidans* with complex of PVA and sodium alginate. Polym. Degrad. Stab. 91, 2408–2414.

Yujian, W., Xiaojuan, Y., Wei, T., Hongyu, L., 2007. High-rate ferrous iron oxidation by immobilized *Acidithiobacillus ferrooxidans* with complex of PVA and sodium alginate. J. Microbiol. Methods 68, 212–217.

Zhang, J., Yuan, Y., Shen, J., Lin, S., 2003. Synthesis and characterization of chitosan grafted poly(*N*; *N*-dimethyl-*N*-methacryloxyethyl-*N*-(3-sulfopropyl) ammonium) initiated by ceric (IV) ion. Eur. Polym. J. 39, 847–850.